JVST A
Journal of Vacuum Science & Technology A

Challenges in atomic layer etching of gallium nitride using surface oxidation and ligand-exchange

Cite as: J. Vac. Sci. Technol. A **41**, 022603 (2023); https://doi.org/10.1116/6.0002255
Submitted: 28 September 2022 • Accepted: 23 January 2023 • Published Online: 01 March 2023

Daniel C. Messina, Kevin A. Hatch, Saurabh Vishwakarma, et al.

JVST A
Journal of Vacuum Science & Technology A

ARTICLE

avs.scitation.org/journal/jva

Challenges in atomic layer etching of gallium nitride using surface oxidation and ligand-exchange

Cite as: J. Vac. Sci. Technol. A 41, 022603 (2023); doi: 10.1116/6.0002255
Submitted: 28 September 2022 · Accepted: 23 January 2023 ·
Published Online: 1 March 2023

Daniel C. Messina,[1] Kevin A. Hatch,[1] Saurabh Vishwakarma,[1] David J. Smith,[1] Yuji Zhao,[2,3] and Robert J. Nemanich[1,a)]

AFFILIATIONS

[1]Department of Physics, Arizona State University, Tempe, Arizona 85287-1504
[2]School of Electrical, Computer, and Energy Engineering, Arizona State University, Tempe, Arizona 85287-8806
[3]Department of Electrical and Computer Engineering, Rice University, Houston, Texas 77005

Note: This paper is part of the 2023 Special Topic Collection on Atomic Layer Etching (ALE).
a)Author to whom correspondence should be addressed: robert.nemanich@asu.edu

ABSTRACT

Two atomic layer etching (ALE) methods were studied for crystalline GaN, based on oxidation, fluorination, and ligand exchange. Etching was performed on unintentionally doped GaN grown by hydride vapor phase epitaxy. For the first step, the GaN surfaces were oxidized using either water vapor or remote O_2-plasma exposure to produce a thin oxide layer. Removal of the surface oxide was addressed using alternating exposures of hydrogen fluoride (HF) and trimethylgallium (TMG) via fluorination and ligand exchange, respectively. Several HF and TMG super cycles were implemented to remove the surface oxide. Each ALE process was monitored *in situ* using multiwavelength ellipsometry. X-ray photoelectron spectroscopy was employed for the characterization of surface composition and impurity states. Additionally, the thermal and plasma-enhanced ALE methods were performed on patterned wafers and transmission electron microscopy (TEM) was used to measure the surface change. The x-ray photoelectron spectroscopy measurements indicated that F and O impurities remained on etched surfaces for both ALE processes. Ellipsometry indicated a slight reduction in thickness. TEM indicated a removal rate that was less than predicted. We suggest that the etch rates were reduced due to the ordered structure of the oxide formed on crystalline GaN surfaces.

I. INTRODUCTION

Gallium nitride (GaN) is an emerging semiconducting material with applications for power electronics owing to its wide bandgap (~3.4 eV), high critical electric field (>3 MV/cm), electron mobility (~2000 $cm^2 V^{-1} s^{-1}$), and dielectric constant (~9).[1,2] These properties make GaN attractive for power conversion and fast switching with smaller volumes in comparison to their silicon ($E_g = 1.1$ eV, $E_{crit} = 0.6$ MV/cm, $\mu = 1200$ $cm^2 V^{-1} s^{-1}$, $\kappa \sim 12$) or silicon carbide (4H-SiC) ($E_g = 3.3$ eV, $E_{crit} = 3.0$ MV/cm, $\mu = 800$ $cm^2 V^{-1} s^{-1}$, $\kappa \sim 10$) counterparts.[3–5] Development of GaN-based electronic devices has been limited by their ability to achieve selective-area doping and management of structural and point defects within GaN.[6] Dry etching of GaN, as typically required for device fabrication, may introduce electrically active defects into the material.[7–9] Current leakage and high field breakdown have been observed to be particularly affected in GaN-based devices prepared by reactive ion etching (RIE) or inductively coupled plasma (ICP) etching. Etch-induced defects are most highly concentrated within a few nanometers of the surface and near-surface regions. However, deep damage may also occur, with reported damage extending beyond 50 nm from the wafer surface.[10] The motivation of this study is to employ ALE to remove the near-surface damage and a post-etching process (such as thermal annealing) to mitigate the deeper damage.

Issues with achieving selective-area doping of GaN have led researchers to investigate alternative methods to obtain lateral devices, such as selective-area regrowth of p-type GaN,[11] or the

use of carrier selective contacts.[12] Regrowth methods typically employ dry etching for patterning, further motivating reduction of etch-induced defects in GaN. Mitigation and removal of etch-induced defects has been pursued through development of new etch techniques or postetch treatments.[7–9,13]

Atomic layer etching (ALE) is a self-limiting or pseudo-self-limiting layer removal technique with subnanometer precision.[14,15] ALE achieves self-limiting material removal using sequential exposures of precursors, or reactants, separated by inert gas purges. A model ALE process would consist of a surface modification step and a removal step separated by purging steps.

Previously developed ALE processes for GaN have used thermal and plasma enhanced methods. Plasma enhanced ALE (PEALE) methods have focused on surface modification by thermal or plasma-assisted halogenation (e.g., F, Cl, Br) to produce GaX_3, with X denoting the halide, which is then removed using plasma.[16–20] Similarly, thermal ALE (TALE) processes for GaN have employed alternating exposures of XeF_2 and BCl_3 to enable self-limiting material removal without an ion component.[16]

Our proposed ALE process for GaN is informed by recent TALE methods where atomic layer removal of a modified surface occurs through a ligand-exchange mechanism. The ligand-exchange involves a metal precursor exchanging a ligand with a molecule at the modified surface, producing stable and volatile complexes that desorb from the surface.[21] A surface modifying fluorination step followed by a ligand-exchange step is a commonly used method for thermal ALE of several oxide and nitride materials.[15,21] However, direct fluorination of GaN surfaces has proved difficult as anhydrous HF was demonstrated to be ineffective in GaN ALE with no evidence of material removed over 20 cycles.[16]

An alternative to direct halogenation of GaN is to employ an oxidation step. Recently, ALE processes of Ga_2O_3 have been developed around fluorination and ligand exchange mechanisms. For example, Lee *et al.* showed that Ga_2O_3 can be fluorinated using HF to produce a GaF_3 layer.[22] Removal of the surface fluoride was then demonstrated using various metal precursors. Recently, Hatch *et al.* showed that trimethylgallium (TMG) could also be used to remove the surface GaF_3.[23] Use of TMG as the metal precursor is advantageous for ALE of GaN to avoid introducing residual metals during the process.

The implementation of the GaN ALE process requires self-limiting oxidation of the GaN surface. Low temperature oxidation (<500 °C) of GaN has been demonstrated using a remote O_2/He-plasma, where the surface oxide thickness was dependent on the substrate temperature and the plasma exposure time.[24] Moreover, the remote plasma oxidation did not show morphological changes. Remote plasma oxidation, thus, provides a plasma enhanced method that could enable GaN ALE. A thermal method for oxidizing GaN may employ water vapor exposure. Recent reports indicate that water adsorption onto a GaN (0001) surface by association and dissociation produces ~ 1 monolayer (ML), or ~0.5 nm, of oxide, where 1 ML corresponds to one adsorbed oxygen atom per surface primitive cell.[25,26]

In this study, surface oxidation was adopted as an alternative pathway to fluorinate the GaN surface. This ALE process employs an oxidation, fluorination, and ligand-exchange process sequence. In this work, two multistep processes were implemented for the ALE of GaN (0001), schematically shown in Fig. 1. The two processes differed by the oxidation method and the number of Ga_2O_3 etch cycles required to remove the converted oxide. The two surface oxidation methods were a remote O_2-plasma exposure or a water vapor exposure. The removal of the surface oxide proceeded using the process developed for Ga_2O_3 ALE.[23] During this study, it became evident that the etch processes were less effective than anticipated with minimal material removal observed. Results that describe the structure of the surface oxide are considered in Sec. IV to potentially explain the reduced efficacy of the ALE process.

The GaN ALE processes were monitored using *in situ* ellipsometry and then studied by x-ray photoelectron spectroscopy (XPS). XPS allowed for determination of the surface composition and band bending, which is directly related to defect formation.[13] To gain insight into the removal per cycle, the GaN ALE processes were applied to GaN patterned surfaces suitable for transmission electron microscopy observation of the surface condition after the ALE processes.

II. EXPERIMENT

Atomic layer etching of GaN (0001) surfaces was performed on unintentionally doped (UID) GaN grown on sapphire substrates. The GaN surfaces were cleaned *ex situ* prior to insertion into an ultra-high vacuum (UHV) multichamber system. The UHV multichamber system included a load-locked chamber, a transfer line, a fluoride ALE reactor, an XPS system, and other growth and characterization chambers.[27,28] XPS was performed before and after etching of the unpatterned GaN wafer. Transmission electron microscopy (TEM) measurements were employed on ALE processed GaN surfaces with lithographically defined Au/Ti patterns to identify the original surface.

A. Sample preparation

The PEALE and TALE processes were performed on $15 \times 15\,mm^2$ UID single-side polished GaN (0001) surfaces grown by hydride vapor phase epitaxy (HVPE) (Kyma Technologies, GT.U.100.0050.B). Each sample consisted of $5.0 \pm 0.5\,\mu m$ UID GaN/~170 nm AlN/sapphire (0001). GaN surfaces were cleaned *ex situ* using a 10 min UV O_3 exposure followed by a 10 min HCl dip. Transmission electron microscopy samples were patterned with Ti/Au via photolithography.

B. GaN ALE and surface characterization

GaN surfaces were etched in a custom-built ALD/ALE reactor capable of generating remote radio frequency (RF) inductively coupled plasma (ICP). The ALE reactor has been described previously.[23] The GaN oxidation step employed either an oxygen plasma or a water vapor exposure. The fluorination employed a hydrogen fluoride-pyridine (HF-P) precursor for HF exposures, and the surface fluoride was removed using a trimethylgallium (TMG) precursor. Pyridine partial pressure at room temperature is negligible, enabling delivery of anhydrous HF without the use of pressurized gas cylinders.[22] To avoid reaction with nitrogen, the HF and TMG were delivered with Ar carrier gas and the purge steps also employed Ar. The purge flow rates were chosen to prevent precursors from

backflowing into the chamber. Reactor pressure was dynamically controlled using exhaust throttling, and the chamber pressure was recorded using a custom LABVIEW program at 1 s intervals.

Plasma excitation was achieved using 13.56 MHz RF applied to a 13-turn copper coil wound around a 32 mm diameter fused quartz tube. The quartz tube extended into the ALE reactor to ~25 cm above the sample surface. This configuration allowed for the generation of a remote RF plasma with high concentrations of thermalized plasma generated radicals and a low concentration of ions.[29,30]

The ALE cycles were structured in a $A_n(BC)_m$ format where A, B, and C denote reactant steps, while m and n denote the number of repetitions. Each reactant step included an inert gas purge. Here, A represents the oxidation step with either a remote oxygen plasma (PEALE) or a water vapor exposure (TALE). B and C represent the HF and TMG reaction steps, respectively. XPS and *in situ* ellipsometry were used to determine m, the sufficient number of B and C repetitions for oxide removal. For the PEALE case, each O_2-plasma exposure required ten HF and TMG steps, or $A_1(BC)_{10}$. For TALE, each water vapor exposure was followed by five alternating HF and TMG step; the process structure was $A_1(BC)_5$. Further discussion of the use of super cycles to remove oxidation may be found in the supplementary material.[46]

For both the TALE and PEALE processes, HF and TMG were each pulsed for 0.1 s into an Ar carrier gas with flow rate 2.0 SCCM, followed by a 30 s exposure and 30 s N_2 purge. The pressure transients were approximately 800 and 200 mTorr during HF, and TMG exposures, respectively. For the TALE process, H_2O was pulsed for 0.1 s into an Ar carrier gas with a flow rate of 2.0 SCCM, followed by a 30 s exposure with pressure transient of 300 mTorr and a 30 s N_2 purge. For PEALE, O_2 was pulsed into the chamber as the pressure stabilized to 100 mTorr over 5 s. The plasma was ignited at 100 W for 10 s, after which the chamber was purged with N_2 for 30 s. In previous experiments, the resulting surface oxide thickness was measured to be ~1.0 nm. The duration of each $A_n(BC)_m$ super cycle in TALE and PEALE was ~13 and ~25 min, respectively.

XPS was employed to gain insight into surface film composition and defect configurations. The XPS instrument (VG Scienta, R3000) used a monochromatic Al Kα source with a photon energy of 1486.7 eV. Data acquisition was performed using the manufacturer supplied software (VG Scienta, SES Software). The system pressure was below 7×10^{-10} Torr during measurements. Survey and high-resolution narrow scans were taken. Scans had an energy resolution of 0.15 eV and a step size of 0.05 eV. Peak analysis was performed using an XPS software package (CASA SOFTWARE LTD, CasaXPS). XPS intensities were normalized using the corresponding photoionization cross section.[31] Surface composition was determined using a standard method which has an accuracy between 10% and 20%.[31–33]

In situ multiwavelength ellipsometry (MWE) was used for process monitoring during processing. The MWE (Film Sense, FS-1) uses four light-emitting diodes (LED) centered at 465, 525, 580, and 635 nm. The ellipsometer was mounted at a fixed angle of ~45°. The ellipsometer determined the polarization state of the reflected beams by the division-of-amplitude-polarimeter (DOAP) method, where all four Stokes parameters were measured simultaneously.[34] Measurements were taken using the manufacturer supplied software (Film Sense, Desktop v1.15) at 1 s intervals. Due to the thickness of the GaN samples, the ellipsometer could not resolve the thicknesses of removed layers. Ellipsometry is, therefore, presented in terms of the ellipsometric parameter Δ for the blue LED as Δ is the most surface sensitive.[35,36] For a heterogeneous structure, increases in Δ are associated with decreases in film thickness and vice versa. However, changes of surface species or plasma ignition may also cause changes in the signal interpreted as changes in Δ. Therefore, changes in Δ may not be completely representative of the film thickness.

Samples suitable for cross-sectional TEM observation were prepared by focused ion beam (FIB) (Thermo Fisher Scientific, Helios 5 UX dual beam system) initially operated at 30 kV, with further thinning at 5 kV, and final cleaning at 2 kV. High-resolution TEM images were recorded using a field emission analytical electron microscope (JEOL, JEM 2010F) operated at 200 kV and with an aberration corrected TEM (FEI, Titan 80-300) operated at 300 kV.

III. RESULTS

Two oxidation methods (O_2 plasma and H_2O) were implemented on GaN (0001) surfaces to enable atomic layer etching. The unpatterned surfaces were initially treated with a 10 min UV-O_3 exposure followed by a 10 min HCl dip prior to insertion into the UHV transfer line. X-ray photoelectron spectra of the GaN surfaces were measured after the following: (1) the initial *ex situ* clean, (2) an *in situ* remote O_2-plasma, (3) 10 alternating HF and TMG exposures, (4) two super cycles of GaN PEALE, and (5) four super cycles of GaN TALE. *In situ* ellipsometry was measured during an initial O_2-plasma exposure followed by 10 alternating exposures of

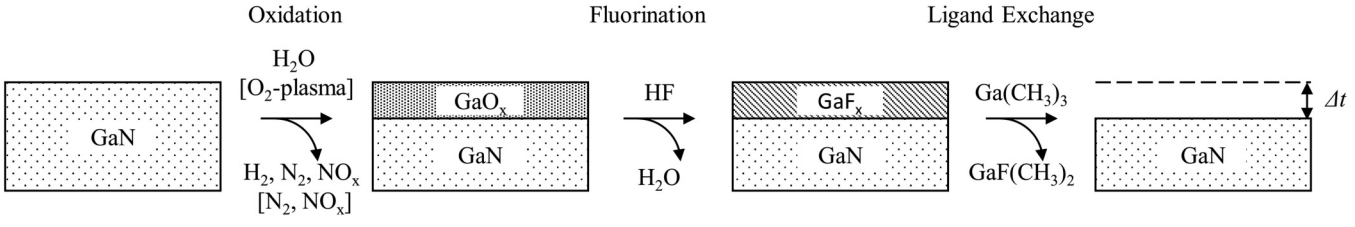

FIG. 1. Schematic illustration of the GaN ALE processes. GaN was oxidized either using water vapor or remote O_2-plasma exposure to create a thin surface oxide. The surface oxide was removed using a Ga_2O_3 ALE process consisting of HF and TMG exposure.

HF and TMG, and during the PEALE and TALE processes. Finally, TEM images of three samples are shown. TEM was performed on a control sample along with PEALE and TALE samples. The TALE process employed twice the number of super cycles to obtain a projected similar etch removal thickness (<2 nm).

A. X-ray photoelectron spectroscopy

The x-ray photoelectron spectra obtained after each step of the ALE processes are shown in Fig. 2. After the *ex situ* clean, the O 1 s and C 1 s spectra indicated the initial surface had a native oxide and a small amount of adventitious carbon. The GaN samples were then exposed to a remote O_2-plasma (100 mTorr at 100 W for 10 s) to clean and oxidize the surface. The resulting O_2-plasma processed surface [Fig. 2(ii)] showed carbon impurities near the detection limit. Broadening of the O 1 s Ga-O peak was observed which was interpreted as indicating multiple oxide configurations. Relative to the other process steps, the O_2-plasma exposed surface showed a shift to lower binding energies indicating a change of band bending, which is consistent with previous reports.[24,37,38]

After the O_2-plasma, ten alternating HF and TMG steps were performed to remove the converted oxide; the XPS scans are shown in Fig. 2(iii). The spectra indicated that a small amount of carbon remained on the surface, which is interpreted as unreacted methyl

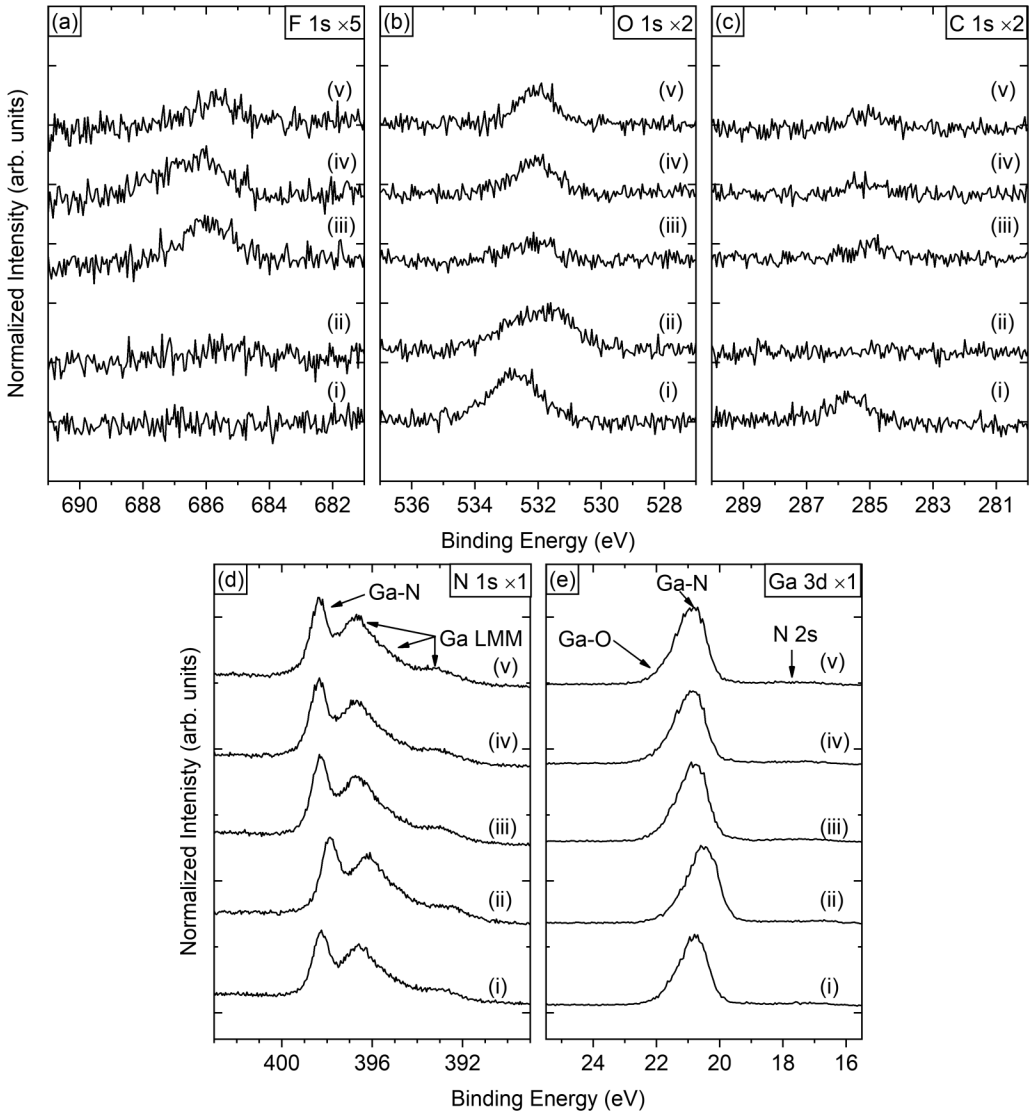

FIG. 2. (a) F 1s, (b) O 1s, (c) C 1s, (d) N 1s, and (e) Ga 3d core levels of the GaN (0001) surfaces after different process steps: (i) *ex situ* cleaned surface, (ii) O_2-plasma exposure, (iii) ten alternating exposures of HF and TMG, (iv) two super cycles of Gan PEALE, and (v) four super cycles of GaN TALE.

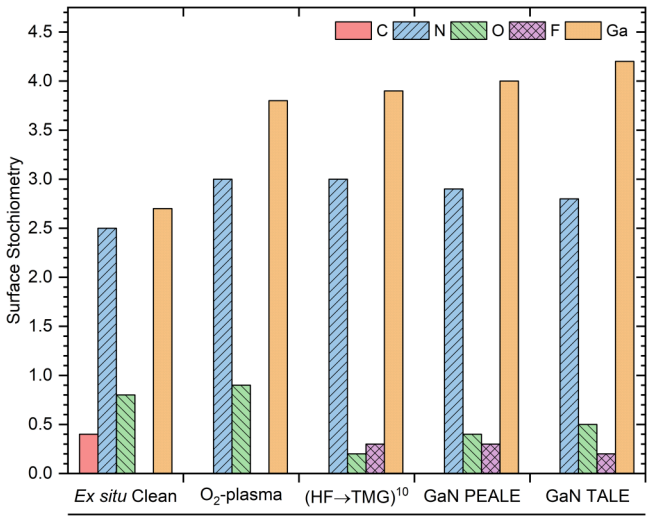

FIG. 3. Surface stoichometry (as determined from XPS measurements) after each process step.

groups.[33] The carbon signal was too weak for more detailed analysis. The O 1 s spectrum showed a decrease in O concentration. Additionally, fluorine was detected on the surface, which is assumed to indicate the presence of GaF_x.[39] After the ten alternating HF and TMG steps, the band bending reverted to the initial state.

The surface stoichiometry was calculated from the XPS for each process step and shown in Fig. 3. The *ex situ* cleaned surface indicated the N:Ga ratio was roughly equal. After the O_2-plasma and removal of hydrocarbon impurities, the surface was more Ga-rich. Additionally, the oxygen concentration remained almost constant. After application of ten HF-TMG cycles, the oxygen concentration decreased by ~74% and fluorine remained on the surface accounting for ~0.3 at. %. After each ALE process, slight changes in the oxygen and fluorine concentrations were observed. Interestingly, the N:Ga ratio was relatively constant through each step excluding the initial *ex situ* clean. The C 1 s peak intensities in Fig. 3 were too close to the XPS detection limit for analysis.

B. Ellipsometry

In situ ellipsometry scans during the GaN PEALE and TALE processes are shown in Fig. 4. The ellipsometry results are

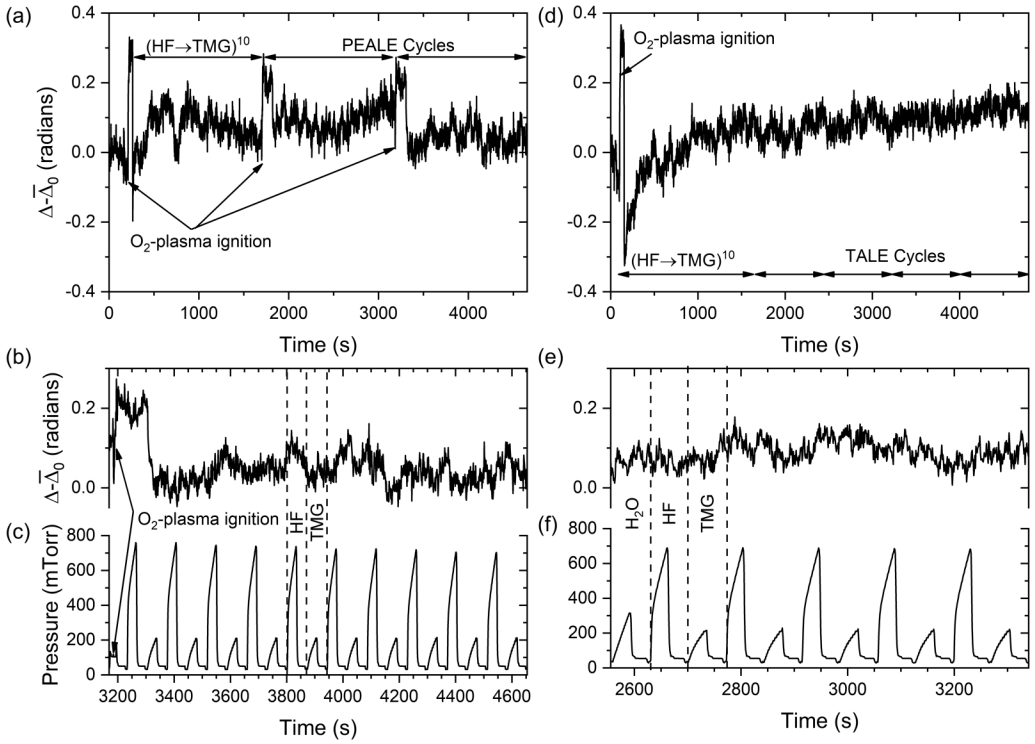

FIG. 4. *In situ* ellipsometry scans during the GaN PEALE and TALE processes. In (a–c) and (d–f), the PEALE and TALE processes are shown, respectively. In (a) and (d), the full ALE processes are shown. The ellipsometry ($\Delta - \bar{\Delta}_0$) and the process pressure for the second PEALE cycle is shown in (b) and (c), respectively. In (e) and (f), the ellipsometry and process pressure are shown for the third TALE cycle.

presented in terms of the change in the ellipsometric parameter Δ with respect to the average of Δ over an initial period of 60 s prior to the process start, $\bar{\Delta}_0$. For each ALE process, a remote O_2-plasma exposure was applied, which was followed by ten alternating HF and TMG steps. Upon the ignition of each O_2-plasma, a large increase in Δ was observed. The increase due to an O_2-plasma ignition lasted ∼2 min during which the first HF step occurred, Figs. 4(b) and 4(c). The small 0.05–0.1 change in $\Delta - \bar{\Delta}_0$ indicates the absence of a surface oxide or accumulation of etch impurities (for either ALE process).

C. Transmission electron microscopy

A set of three samples prepared for transmission electron microscopy included a GaN control sample and two GaN surfaces patterned with metal contacts. The patterned GaN surfaces were subjected to either 5 or 10 super cycles of the PEALE and TALE process, respectively. Etch per super cycle (EPC) was assumed from oxidized GaN surface XPS and MWE measurements to be 1 and 0.5 nm for PEALE and TALE, respectively. The number of cycles was then chosen such that a thickness of 5 nm would be removed for both processes. After the processes were completed, cross-sectional TEM was performed on each sample and results are shown in Fig. 5. The control sample is shown in Figs. 5(a) and 5(b). In Fig. 5(b), some surface fringes are observed indicating some surface roughness. The PEALE sample is shown in Figs. 5(c) and 5(d). Figure 5(c) shows the area under a metal contact adjacent to an area exposed to the PEALE process. The PEALE process removed less GaN than anticipated, which is estimated to be less than 2 nm. An area similar to Fig. 5(c) for the TALE process is shown in Fig. 5(e). Like the PEALE sample, the TALE sample does not show clear evidence of GaN etching (through comparison of the surface under and adjoining the metal regions). Similar to the control sample, fringes are observed in Fig. 5(d) indicating surface roughness but to a lesser extent than Fig. 5(b). A minor difference between the two processes is that the TALE exposed area, Fig. 5(f), shows fewer surface fringes possibly indicating reduced surface roughness in these areas.

IV. DISCUSSION

XPS measurements indicated that O_2 plasma resulted in oxidation of ∼1.0 nm of the GaN surface, while HF exposure reduced the oxide while fluorinating the surface, as expected. However, a reduction of the oxide was not complete as O was still observed in the XPS measurements. XPS and ellipsometry measurements indicated an oxidized surface remained after one cycle of O_2 plasma, HF, and TMG exposures. Repeated cycles produced oxide accumulation at the GaN surface. To compensate for this accumulation, multiple exposures of HF and TMG were employed to more fully remove the oxide formed at the surface. The application of alternating exposures of HF and TMG per each plasma oxidation prevented oxide accumulation, allowing for ALE super cycles to

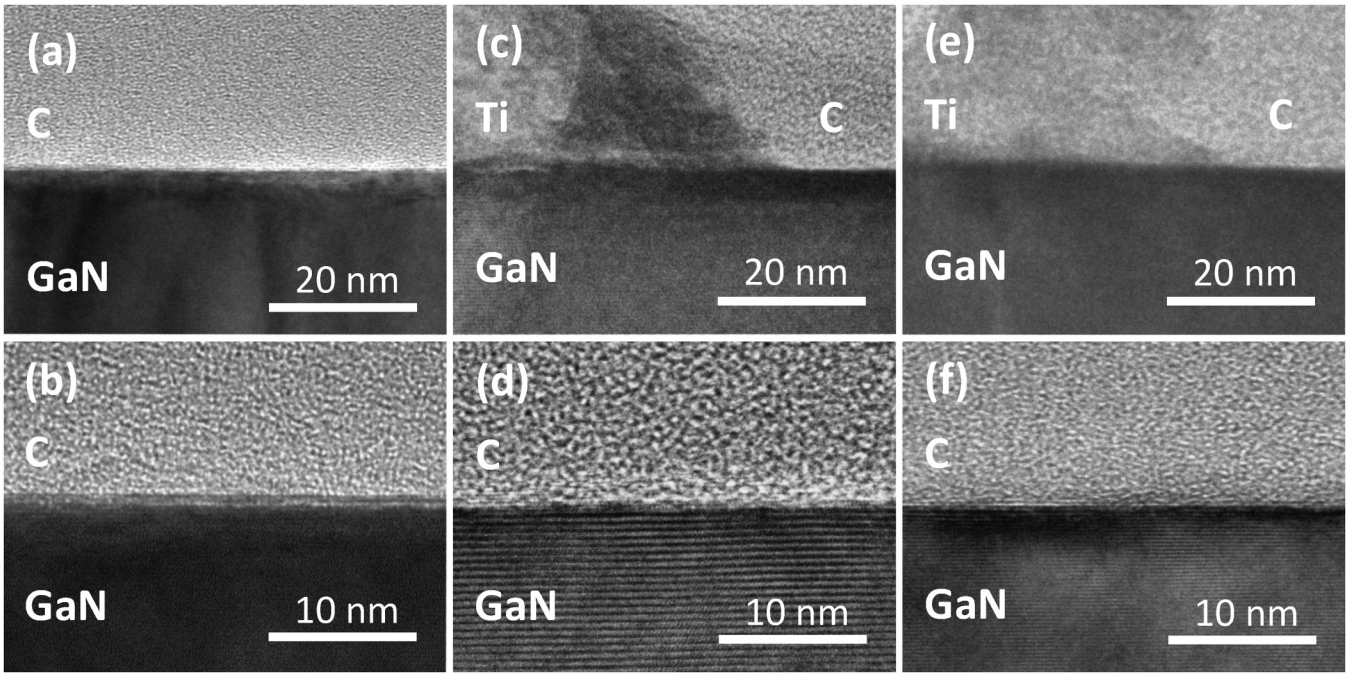

FIG. 5. Transmission electron microscopy of the [(a) and (b)] control sample, [(c) and (d)] the plasma oxidized, and [(e) and (f)] thermally oxidized GaN samples. The control sample had no patterning. (c) and (e) show the edge of the metal contact (Ti), while (d) and (f) are well away from the contact.

effectively etch GaN. See the supplementary material[46] for further discussion of oxide accumulation and ALE super cycles.

The ellipsometry results indicated small decreases in thickness for both the PEALE and TALE processes. However, the change in Δ of this scale (>0.1) could indicate either etching or a change in surface roughness. The excess thickness of MOCVD GaN samples obscured MWE measurement of the etch removal thickness. Increased exposures of HF and TMG prevented oxide accumulation, resulting in a constant thin oxide layer as observed by MWE over multiple super cycles.

From previous reports and initial measurements, the water vapor and O_2-plasma exposures were expected to produce ∼0.5 and ∼1.0 nm of GaO_x, respectively. Over the 5 or 10 super cycles of PEALE and TALE, respectively, an etched thickness of ∼5 nm was expected. Etching was performed on patterned surfaces for characterization using TEM. However, TEM observations indicated that the etch rate by both ALE processes was lower than expected and a more precise change in thickness could not be determined. These results may be interpreted as a maximum of only 1–2 nm reduction in thickness over the 5 or 10 super cycles, and seem to be lower for the TALE GaN. Surface fringes observed in TEM images of the ALE GaN suggested lower surface roughness than for the control sample, indicating that ALE produced smoothing of the GaN surface.

These results suggest the converted oxide could not be effectively etched using HF and TMG. This may be due to crystallinity of the oxide. As noted by Dycus *et al.* the native oxide on GaN (0001) can be highly ordered in an arrangement similar to β-Ga_2O_3.[40] Additionally, Hao *et al.* showed that crystalline β-Ga_2O_3 can be grown on GaN by plasma enhanced atomic layer deposition (PEALD) at only 250 °C (i.e., the temperature used in this study).[41] See the supplementary material[46] for further discussion of oxide crystallinity on GaN.

HF and TMG have been shown to be effective for ALE of Ga_2O_3.[20] However, studies of ALE of crystalline AlN and Al_2O_3 suggest that the crystalline III-nitrides and III-oxides may be more difficult to etch thermally using HF when compared with amorphous materials. Johnson *et al.* reported a method for thermal ALE of crystalline AlN using HF and $Sn(acac)_2$.[42] In this study, wurtzite AlN (0001) was etched, and an XPS depth profile indicated the presence of a 4 nm AlO_xN_y layer at the AlN surface. Thermal ALE produced an etch rate of only 0.07 Å/cycle for the AlO_xN_y layer compared to 0.36 Å/cycle for the underlying AlN. Additionally, Murdzek *et al.* showed that negligible etching of crystalline Al_2O_3 occurred beyond the initial 10 Å from the surface, when using HF and trimethylaluminum (TMA).[43]

ALE using O_2 plasma has recently been reported in a fully plasma-based ALE process of GaN using BCl_3 plasma as the other reactant, which indicates removal of the converted oxide is possible.[44] Although, it remains to be seen if there is a thermal pathway for removal. Future studies could investigate ALE of crystalline β-Ga_2O_3 using HF and TMG, as well as other thermal chemistries, as successful thermal ALE processes for crystalline Ga_2O_3 may prove effective in etching the converted oxide on GaN.

Alternatively, future studies could incorporate a high temperature (≥750 °C) NH_3 or H_2/N_2 anneal to remove the native oxide prior to application of the TALE and PEALE method.[45] Oxidation at different substrate temperatures could then be investigated to produce a less ordered surface oxide, which may improve removal rates using thermal reactions. Additionally, modulation of the O_2-plasma composition to include Ar or He may be beneficial for producing an amorphous surface oxide.[24,37,38]

V. SUMMARY AND CONCLUSIONS

This study investigated oxidation as a pathway for ALE of GaN using O_2 plasma, HF, and TMG. Two ALE methods for gallium nitride have been presented. These methods differed in the oxidation method, using either water vapor or remote O_2-plasma exposure. Both methods were studied by *in situ* ellipsometry, XPS, and *ex situ* TEM. Ellipsometry results indicated a small change in Δ which could be interpreted as a small change in thickness. XPS showed the etch processes left a small amount of impurities (F, O, C) on the surface accounting for 8–10 at. % of the surface composition. TEM of etched patterned samples indicated that a maximum of 1–2 nm of GaN had been removed. Additionally, a slight reduction in surface roughness was observed relative to a control sample. TEM results indicated ALE produced smoothing of the surface. However, the etch rate using this method was smaller than predicted. This low etch rate is attributed to a highly ordered native oxide formation on GaN producing decreased etch activity from thermal reactions. Alternative oxidation methods or different substrate temperatures during oxidation may be investigated which would produce a disordered surface oxide and consequently improved ALE reactions.

ACKNOWLEDGMENTS

Research was supported through the Advanced Research Projects Agency-Energy, as part of PNDIODES, under Grant No. DE-AR0000868 (research on thermal oxidation and analysis of TALE GaN) and by the U.S. Department of Energy (DOE), Office of Science, as part of ULTRA, an energy Frontier Research Center funded by Basic Energy Sciences (BES), under Award No. DE-SC0021230 (research on plasma oxidation and analysis of PEALE GaN). We acknowledge the use of facilities within the John. M. Cowley Center for High Resolution Electron Microscopy and the NanoFab, at Arizona State University, supported in part by the NSF Program No. NNCI-ECCS-1542160. We acknowledge Kari Slotten for patterning the GaN samples and Martha McCartney for assistance with TEM. We thank Franz Koeck for assistance in assembling the fluoride ALE reactor and to Zhiyu Huang, Jesse Brown, Avani Patel, Xingye Wang, and Mei Hao for their helpful discussions.

AUTHOR DECLARATIONS

Conflict of Interest

The authors have no conflicts to disclose.

Author Contributions

D. C. Messina: Conceptualization (equal); Formal analysis (equal); Investigation (equal); Writing – original draft (equal); Writing – review & editing (equal). **K. A. Hatch:** Conceptualization (equal);

Formal analysis (equal); Investigation (equal); Writing – original draft (equal); Writing – review & editing (equal). **S. Vishwakarma:** Formal analysis (supporting); Investigation (supporting). **D. J. Smith:** Conceptualization (supporting); Resources (supporting); Supervision (supporting). **Y. Zhao:** Conceptualization (supporting); Funding acquisition (lead); Supervision (supporting). **R. J. Nemanich:** Conceptualization (equal); Resources (equal); Supervision (equal); Writing – review & editing (equal).

DATA AVAILABILITY

The data that support the findings of this study are available from the corresponding author upon reasonable request.

REFERENCES

[1]B. J. Baliga, Semicond. Sci. Tech. **28**, 074011 (2013).
[2]Y. Zhang, A. Dadgar, and T. Palacios, J. Phys. D: Appl. Phys. **51**, 273001 (2018).
[3]S. Chowdhury, Phys. Stat. Sol. A **212**, 1066 (2015).
[4]J. Tian, C. Lai, G. Feng, D. Banerjee, W. Li, and N. C. Kar, Int. J. Sustain. Energy **39**, 88 (2020).
[5]M. J. Scott, L. Fu, X. Zhang, J. Li, C. Yao, M. Sievers, and J. Wang, Semicond. Sci. Tech. **28**, 074013 (2013).
[6]H. Fu *et al.*, Mater. Today **49**, 296 (2021).
[7]J. M. Lee, K. M. Chang, S. W. Kim, C. Huh, I. H. Lee, and S. J. Park, J. Appl. Phys. **87**, 7667 (2000).
[8]Z. Mouffak, A. Bensaoula, and L. Trombetta, J. Appl. Phys. **95**, 727 (2004).
[9]R. J. Shul, L. Zhang, A. G. Baca, C. G. Willison, J. Han, S. J. Pearton, K. P. Lee, and F. Ren, Solid State Electron. **45**, 13 (2001).
[10]X. A. Cao *et al.*, Appl. Phys. Lett. **75**, 232 (1999).
[11]A. Debald, S. Kotzea, M. Heuken, H. Kalisch, and A. Vescan, Phys. Status Solidi A **216**, 1800677 (2019).
[12]I. Kim, C. Kauppinen, I. Radevici, P. Kivisaari, and J. Oksanen, Phys. Stat. Sol. A **219**, 2100461 (2022).
[13]K. A. Hatch, D. C. Messina, H. Fu, K. Fu, Y. Zhao, and R. J. Nemanich, J. Appl. Phys. **131**, 185301 (2022).
[14]K. J. Kanarik, T. Lill, E. A. Hudson, S. Sriraman, S. Tan, J. Marks, V. Vahedi, and R. A. Gottscho, J. Vac. Sci. Technol. A **33**, 020802 (2015).
[15]A. Fischer, A. Routzahn, S. M. George, and T. Lill, J. Vac. Sci. Technol. A **39**, 030801 (2021).
[16]N. R. Johnson, J. K. Hite, M. A. Mastro, C. R. Eddy, and S. M. George, Appl. Phys. Lett. **114**, 243103 (2019).
[17]C. Kauppinen, S. A. Khan, J. Sundqvist, D. B. Suyatin, S. Suihkonen, E. I. Kauppinen, and M. Sopanen, J. Vac. Sci. Technol. A **35**, 060603 (2017).
[18]C. Mannequin, C. Vallée, K. Akimoto, T. Chevolleau, C. Durand, C. Dussarrat, T. Teramoto, E. Gheeraert, and H. Mariette, J. Vac. Sci. Technol. A **38**, 032602 (2020).
[19]Y. Zhang *et al.*, IEEE Electr. Device Lett. **41**, 701 (2020).
[20]D. Ohori, T. Sawada, K. Sugawara, M. Okada, K. Nakata, K. Inoue, D. Sato, and S. Samukawa, J. Vac. Sci. Technol. A **39**, 042601 (2021).
[21]S. M. George, Acc. Chem. Res. **53**, 1151 (2020).
[22]Y. Lee, N. R. Johnson, and S. M. George, Chem. Mater. **32**, 5937 (2020).
[23]K. A. Hatch, D. C. Messina, and R. J. Nemanich, J. Vac. Sci. Technol. A **40**, 042603 (2022).
[24]C. Bae and G. Lucovsky, J. Vac. Sci. Technol. A **22**, 2402 (2004).
[25]H. Ye, G. Chen, H. Niu, Y. Zhu, L. Shao, and Z. Qiao, J. Phys. Chem. C **117**, 15976 (2013).
[26]M. Sato, Y. Imazeki, T. Takeda, M. Kobayashi, S. Yamamoto, I. Matsuda, J. Yoshinobu, Y. Nakano, and M. Sugiyama, J. Phys. Chem. C **124**, 12466 (2020).
[27]S. W. King, R. F. Davis, R. J. Carter, T. P. Schneider, and R. J. Nemanich, J. Vac. Sci. Technol. A **33**, 05E115 (2015).
[28]Y. Yang, T. Sun, J. Shammas, M. Kaur, M. Hao, and R. J. Nemanich, J. Appl. Phys. **118**, 165310 (2015).
[29]H. B. Profijt, S. E. Potts, M. C. M. van de Sanden, and W. M. M. Kessels, J. Vac. Sci. Technol. A **29**, 050801 (2011).
[30]H. C. M. Knoops, T. Faraz, K. Arts, and W. M. M. Kessels, J. Vac. Sci. Technol. A **37**, 030902 (2019).
[31]J. H. Schofield, J. Electron Spectrosc. **8**, 129 (1976).
[32]F. A. Stevie and C. L. Donley, J. Vac. Sci. Technol. A **38**, 063204 (2020).
[33]J. F. Moulder, W. F. Stickle, P. E. Sobol, and K. D. Bomben, in *Handbook of X-Ray Photoelectron Spectroscopy*, edited by J. Chastain (Perkin-Elmer Corporation Eden Prairie, Minnesota, 1992).
[34]R. M. A. Azzam, Opt. Acta **29**, 685 (1982).
[35]J. B. Theeten and D. E. Aspnes, Ann. Rev. Mater. Sci. **11**, 97 (1981).
[36]A. V. Tikhonravov, M. K. Trubetskov, E. Masetti, A. V. Krasilnikova, and I. V. Kochikov, Proc. SPIE **3738**, 173 (1999).
[37]T. Yamamoto *et al.*, Jpn. J. Appl. Phys. **57**, 06JE01 (2018).
[38]T. Yamamoto *et al.*, Jpn. J. Appl. Phys. **57**, 06KA05 (2018).
[39]V. M. Bermudez, Appl. Surf. Sci. **119**, 147 (1997).
[40]J. H. Dycus, K. J. Mirrielees, E. D. Grimley, R. Kirste, S. Mita, Z. Sitar, R. Collazo, D. L. Irving, and J. M. LeBeau, ACS Appl. Mater. Interfaces **10**, 10607 (2018).
[41]H. Hao *et al.*, J. Semicond. **40**, 012806 (2019).
[42]N. R. Johnson, H. Sun, K. Sharma, and S. M. George, J. Vac. Sci. Technol. A **34**, 050603 (2016).
[43]J. A. Murdzek, A. Rajashekhar, R. S. Makala, and S. M. George, J. Vac. Sci. Technol. A **39**, 042602 (2021).
[44]I. H. Hwang, H. Y. Cha, and K. S. Seo, Coatings **11**, 268 (2021).
[45]V. M. Bermudez, Surf. Sci. Rep. **72**, 147 (2017).
[46]See supplementary material at https://www.scitation.org/doi/suppl/10.1116/6.0002255 for further data and discussion of oxidation and oxide removal at the GaN surface.